Direct Torque Control and MPPT Strategy of PMSG Used for Variable Speed Wind Energy Conversion System

Y. Errami, M. Maaroufi and M. Cherkaoui
Ecole Mohammadia d'Ingénieur, Mohammed V- Agdal University, Department of Electrical Engineering, Rabat, Morocco
errami.emi@gmail.com, maaroufi@emi.ac.ma

M. Ouassaid
Ecole Nationale des Sciences Appliquées- Safi, Cadi Ayyad University, Department of Industrial Engineering, Safi, Morocco
ouassaid@emi.ac.ma

Abstract— **The paper presents a variable speed controller for Permanent Magnet Synchronous Generator (PMSG) in Wind Energy Conversion System (WECS). A Direct Torque Control (DTC) algorithm-based controller is proposed for the PMSG. Generator torque reference is derived based on Maximum Power Point Tracking strategy (MPPT). The block diagram of the WECS with PMSG and the grid-side back-to-back converter is established with the dq frame of axes. A speed controller is designed to maximize the extracted energy from the wind, below the rated power area. A pitch control scheme for variable speed wind turbines is proposed in order to limit the output power produced by the turbine, while the DTC strategy is used to control the generator rotor speed. The objectives of grid-side converter are to deliver the energy from the PMSG side to the utility grid, to regulate the DC-link voltage and to achieve unity power factor and low distortion currents. So, Direct Power Control (DPC) of three phases PWM inverter is adopted and Grid-side reactive and active power decoupling method is applied. The employed control strategy can regulate both the reactive and active power independently. Finally, the effectiveness of the novel control strategy is verified by simulation using Matlab/ Simulink environment. Simulation results confirm that the proposed strategy has excellent performance.**

Keywords-WECS; PMSG; MPPT; DTC; DPC; Unity power factor.

I. INTRODUCTION

In recent years, wind energy has widely grown, and nowadays it's the most competitive form of renewable energy. For economical and cleaner energy characteristics, the WECS are getting a lot of attention and they have been increasing rapidly [1-3]. In addition, variable speed WECS have many advantages over fixed speed generation such as operation at maximum power point, higher energy yields, lower component stress and fewer grid connection power peaks. At present, it's becoming the most important and fastest growing application of WECS [3-4]. At present, in terms of the generators for WECS, several types of electric generators are used such as Doubly Fed Induction Generator (DFIG), Induction Generator (IG) and Permanent Magnet Synchronous Generator (PMSG) [3], [5-8]. Recently, with the rapid development of the power semiconductor devices, PMSG is an attractive choice for variable-speed generation system. It doesn't require any external excitation current. Then, it can reduce again weight, losses, costs and maintenance requirements and operate at low speeds [1], [5]. So as to control the WECS, several control schemes have been proposed [3-7]. Two controllers are used, one is the pitch controller for the pitch angle and the other one is used for the power controller regulating the output power. Therefore, there exists a variety of control schemes such as PI control. In addition, control algorithm based on the vector control strategy (VC) has been investigated for both converters with PI control. Thus, decoupling control of active current and reactive current is necessary [4], [8]. The DTC strategy is an alternative to VC for PMSG based WECS. The DTC technique, with Bang-Bang adjustor, can only select one voltage space vector in order to regulate the torque and flux linkage at the same time during one control period [9-11].

In this context, this paper proposes a WECS using a DTC controlled PMSG. The system model includes a wind turbine, a gearbox, a PMSG and the back to back converters with intermediate DC circuit [3-5]. As the voltage and frequency of generator output vary along the wind speed change, the generator-side converter is used to track the maximum wind power and implement DTC for PMSG, while DPC of inverter is used so as to sustain the DC-bus voltage and regulate the grid-side power factor. Therefore, active and reactive powers are controlled respectively by the inverter in grid-side. So, the DC-link provides decoupling between the grid-side inverter and the generator-side converter [3], [5-6].

The remainder of this paper is organized as follows. Section II gives the models of the wind turbine generator and PMSG. In Section III, control of WECS will be presented. Section IV presents and discusses the simulations results. Finally, some conclusions are given in Section V.

II. MATHEMATICAL MODELING OF WECS

A. Model of wind turbine with PMSG

Output aerodynamic power of the wind-turbine is expressed as [1-2]:

$$P_{Turbine} = \frac{1}{2}\rho A C_p(\lambda,\beta)v^3 \quad (1)$$

where, ρ is the air density, A is the area swept by the rotor blades (in m^2), v is the wind speed (in m/s) C_p is the coefficient of power conversion and β is the blade pitch angle (in degrees) . The tip-speed ratio is defined as [3-4]:

$$\lambda = \frac{\omega_t R}{v} \tag{2}$$

where ω_t and R are the shaft speed (in rad/sec) and rotor radium (in m), respectively.

The torque output of the wind turbine T_m is given by:

$$T_m = \frac{1}{2}\rho A C_p(\lambda,\beta)v^3 \frac{1}{\omega_t} \tag{3}$$

The turbine is coupled to the generator through a gearbox. Thus: $\omega_m = G\omega_t$ where ω_m and G are the rotor angular velocity and the gear ratio, respectively. The power coefficient is a nonlinear function of β and the tip-speed ratio λ. If the swept area of the blade and the air density are constant, the value of C_p is a function of λ and it is maximum at the particular λ_{opt} [1-3]. Hence, to fully utilize the wind energy, λ should be maintained at λ_{opt}, which is determined from the blade design.

A generic equation is used to model the power coefficient $C_p(\lambda,\beta)$ based on the modeling turbine characteristics described in [1] as:

$$C_p = \frac{1}{2}\left(\frac{116}{\lambda_i} - 0.4\beta - 5\right)e^{-\left(\frac{21}{\lambda_i}\right)}$$
$$\frac{1}{\lambda_i} = \frac{1}{\lambda + 0.08\beta} - \frac{0.035}{\beta^3 + 1} \tag{4}$$

The particular value λ_{opt} results in the point of optimal efficiency where the maximum power is captured from wind by the wind turbine. For each wind speed, there exists a specific point in the wind generator power characteristic, MPPT, where the output power is maximized. Thus, the control of the WECS load results in a variable-speed operation of the turbine rotor, so the maximum power is extracted continuously from the wind (MPPT control) [1-2].That's illustrated in Fig.1.

B. *Modelling of PMSG*

Dynamic modelling of PMSG can be described in d-q reference system as follows [4], [8]:

$$v_{gq} = (R_g + pL_q)i_q + \omega_e L_d i_d + \omega_e \psi_f \tag{5}$$

$$v_{gd} = (R_g + pL_d)i_d - \omega_e L_q i_q \tag{6}$$

where v_{gd} and v_{gq} are the direct stator and quadrature stator voltage,respectively. i_d and i_q are the direct stator and quadrature stator current, respectively. R_g is the stator resistance, L_q and L_d are the inductances of the generator on the d and q axis, ψ_f is the permanent magnetic flux and ω_e is the electrical rotating speed of the generator, defined by:

$$\omega_e = p_n \omega_m \tag{7}$$

where p_n is the number of pole pairs of the generator and ω_m is the mechanical angular speed. The expression for the electromagnetic torque can be described as :

$$T_e = \frac{3}{2}p_n\left[\psi_f i_q - (L_d - L_q)i_d i_q\right] \tag{8}$$

If $i_d = 0$, the electromagnetic torque is expressed as[4]:

$$T_e = \frac{3}{2}p_n \psi_f i_q \tag{9}$$

The dynamic equation of the wind turbine is given as:

$$J\frac{d\omega_m}{dt} = T_e - T_m - F\omega_m \tag{10}$$

where J is the moment of inertia , F is the viscous friction coefficient and T_m is the mechanical torque developed by the turbine .

III. THE CONTROL SYSTEM

A. *Adopted MPPT control strategy*

MPPT controller is used so as to generate the reference speed command which will enable the WECS to extract maximum power from the available wind power. When the wind speed changes, the rotational speed is controlled to follow the maximum power point trajectory. So, the optimal rotational speed of the wind turbine rotor can be simply estimated as follows [4], [7]:

$$\omega_{m-opt} = \frac{v\lambda_{opt}}{R} \tag{11}$$

The maximum mechanical output power of the turbine is given as follows:

$$P_{Turbine\_max} = \frac{1}{2}\rho A C_{pmax}\left(\frac{R\omega_{m-opt}}{\lambda_{opt}}\right)^3 \tag{12}$$

Thus, we can get the maximum power $P_{Turbine\_max}$ by regulating the generator speed in different wind speed under rated power of the wind power system. The MPPT controller computes this optimum speed and an optimum value of tip speed ratioλ_{opt} can be maintained and maximum wind power can be captured. In addition, the pitch angle controller is used to keep the WECS operating at rated active power. So, it's only active in high wind speeds and it's designed to prevent generator power exceeding rated power. Therefore, by reducing the coefficient of power conversion, both the power and rated rotor speed are maintained for above rated wind speeds. So, the blade pitch angle, β, will increase until the wind turbine generator is at the rated speed [7-8]. The schematic diagram of the implemented turbine blade pitch angle controller is shown in Fig.2. where P_g is the generated power.

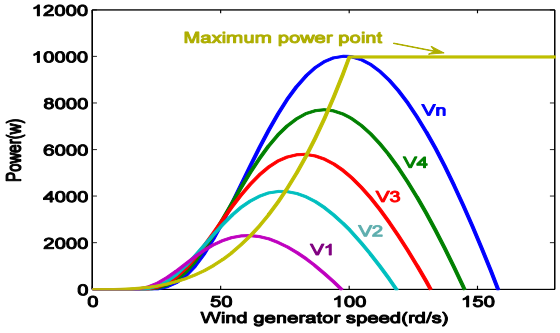

Fig.1. Wind generator power curves at various wind speed.

B. Control of the generator side converter with MPPT and DTC

The generator side rectifier works as a driver controlling the generator operating at optimum rotor speed ω_{m-opt} to obtain maximum energy from wind [5], [7]. So, the MPPT is achived by DTC control. The block diagram of the generator controller is shown in Fig. 3. The PMSG is controlled based on DTC algorithm [9-11]. Generator torque reference is derived based on Maximum Power Point Tracking strategy (MPPT). PI controller is used to regulate the speed of PMSG. The equivalent two-phase stator voltages along the stationary $\alpha-$ axis are obtained as follows [11]:

$$u_{s\alpha} = \frac{U_{dc}}{3}(2S_1 - S_2 - S_3) \quad (13)$$

$$u_{s\beta} = \frac{U_{dc}}{\sqrt{3}}(S_2 - S_3) \quad (14)$$

where $U_{dc}$is the DC-bus voltage and (S_1, S_2, S_3) the switching states of the rectifier. The voltage vectors obtained this way are shown in Fig.4.

The component of the stator flux linkage, in the two phase stationary axis is given [9]:

$$\psi_{s\alpha} = \int (u_{s\alpha} - R_g i_{s\alpha})dt \quad (15)$$

$$\psi_{s\beta} = \int (u_{s\beta} - R_g i_{s\beta})dt \quad (16)$$

The flux amplitude and its phase are derived respectively from:

$$\psi_s = \sqrt{{\psi_{s\alpha}}^2 + {\psi_{s\beta}}^2} \quad (17)$$

$$\theta_s = arctg(\frac{\psi_{s\beta}}{\psi_{s\alpha}} \quad (18)$$

The electromagnetic torque is expressed as:

$$T_e = \frac{3}{2} p_n [\psi_{s\alpha} i_{s\beta} - \psi_{s\beta} i_{s\alpha}] \quad (19)$$

The DTC strategy is based on two discrete hysteretic comparators in witch the stator flux and the torque are controlled directly. The basic principle is that the errors of torque and flux between the reference and feedback values are inputs to the hysteresis controllers in order to select appropriate voltage vector with the help of a pre-defined switching table as shown in Table I. The output of theses comparators(C_ψ, C_T) and the position of stator flux linkage space vector (θ_s) are the three inputs of this switching table. Thus, the vector of voltage makes the flux rotate and produce the desired torque and, with comparators, the amplitude of the flux is kept in a pre-defined band [9-11].

C. Grid-side controller strategy

The objectives of grid-side converter are to deliver the energy from the PMSG side to the utility grid, to regulate the DC-link voltage, to achieve unity power factor [3-5]. Direct Power Control (DPC) is adopted so as to regulate instantaneous values of reactive power and active power of grid connection, respectively [12]. In addition, the input reactive power and active power are decoupling controlled in d-q synchronous reference frame. So, the PI control loops are employed [4], [8]. The controller is shown in Fig. 3. Then, in the inner control loops, reactive and active powers are controlled respectively, while the outer control loop is used for the DC voltage controller. Compensation terms are added as shown in Fig.3, so as to compensate the cross-coupling effect due to the output filter in the synchronous rotating reference frame. In the rotating dq reference frame, the voltage balance across the inductor L_f is given by [4]:

$$L_f \frac{di_{d-f}}{dt} = e_d - R_f i_{d-f} + \omega L_f i_{q-f} - v_d \quad (20)$$

$$L_f \frac{di_{q-f}}{dt} = e_q - R_f i_{q-f} - \omega L_f i_{d-f} - v_q \quad (21)$$

$$C \frac{dU_{dc}}{dt} = \frac{3}{2}\left(\frac{v_d}{U_{dc}} i_{d-f} + \frac{v_q}{U_{dc}} i_{q-f}\right) - i_{dc} \quad (22)$$

where $L_f$and R_f are the filter inductance and resistance respectively; e_d and e_q are the inverter d-axis q-axis voltage components respectively. i_{d-f} ,i_{q-f} are the values of d-axis current and q- axis current, v_d and $v_q$are the grid voltage components in the d-axis q-axis voltage components respectively, U_{dc} is the dc-bus voltage, i_{dc} is the dc-bus current , i_{d-f} and i_{q-f} are the d-axis current and q- axis current of Grid.

The instantaneous power is given by [8]:

$$P = \frac{3}{2}(v_d i_{d-f} + v_q i_{q-f}) \quad (23)$$

$$Q = \frac{3}{2}(v_d i_{q-f} - v_q i_{d-f}) \quad (24)$$

If the grid voltage space vector $\vec{u}$ is oriented on d-axis, then:

$$v_d = V \quad v_q = 0 \quad (25)$$

Thus, equations (20-21) may be expressed as:

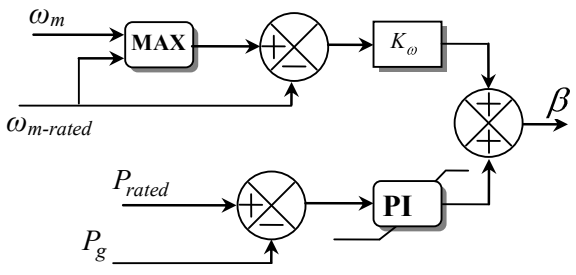

Fig.2. WECS Pitch angle controller.

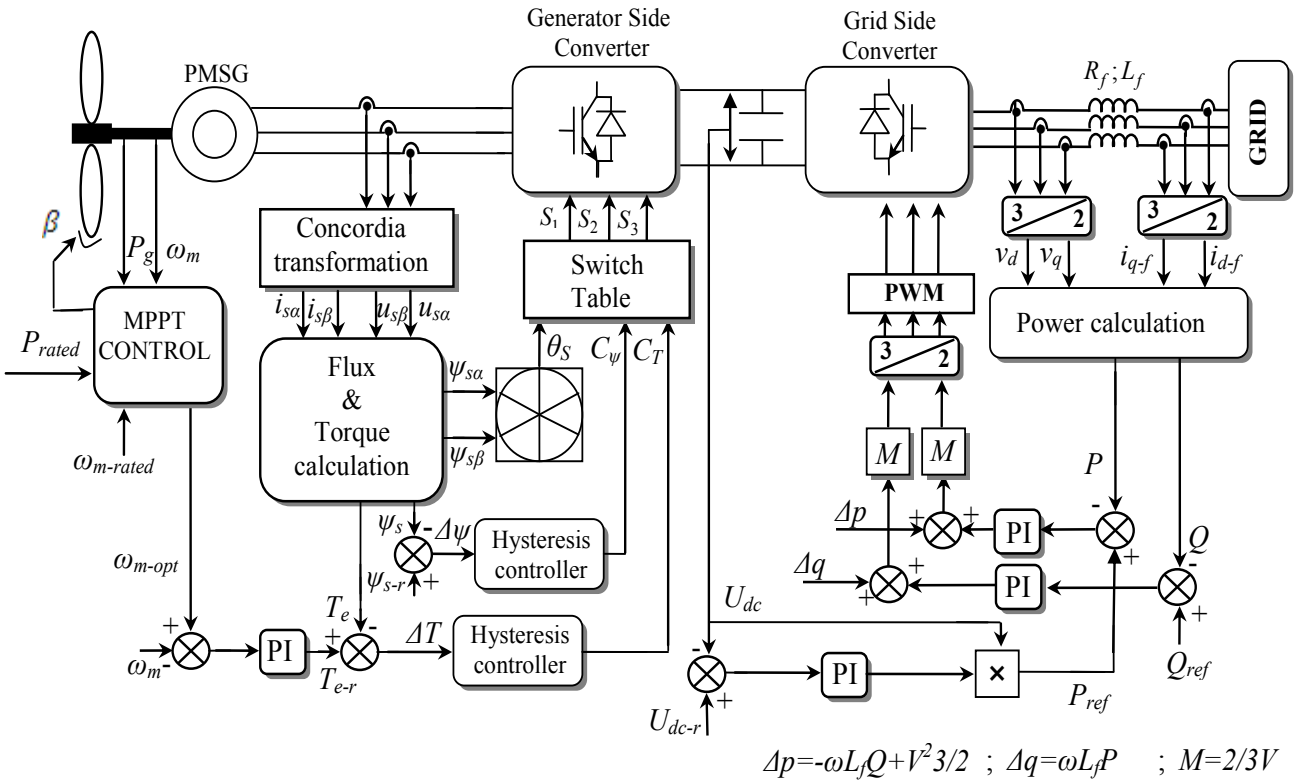

Fig.3. Schematic of Direct Control strategy for WECS based on the PMSG.

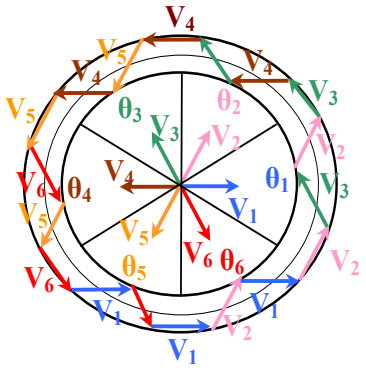

Fig.4. Vectors of space vector modulation.

$$L_f \frac{di_{d-f}}{dt} = e_d - R_f i_{d-f} + \omega L_f i_{q-f} - V \quad (26)$$

$$L_f \frac{di_{q-f}}{dt} = e_q - R_f i_{q-f} - \omega L_f i_{d-f} \quad (27)$$

Then, the reactive power and active power can be expressed as:

$$P = \frac{3}{2} V i_{d-f} \quad (28)$$

$$Q = \frac{3}{2} V i_{q-f} \quad (29)$$

Table I
SWITCHING VECTORS

C_Ψ	C_T	θ_1	θ_2	θ_3	θ_4	θ_5	θ_6
C_Ψ=0	C_T=1	V_3	V_4	V_5	V_6	V_1	V_2
	C_T=0	V_0	V_7	V_0	V_7	V_0	V_7
	C_T= -1	V_5	V_6	V_1	V_2	V_3	V_4
C_Ψ=1	C_T=1	V_2	V_3	V_4	V_5	V_6	V_1
	C_T=0	V_7	V_0	V_7	V_0	V_7	V_0
	C_T= -1	V_6	V_1	V_2	V_3	V_4	V_5

V_1(010); V_2(110); V_3(100) ; V_4(101); V_5(001); V_6(011) ; V_7(111) ; V_0(000)

According to the equation (26), (27), (28) and (29), define the P and Q are the control variables, the power control model can be expressed:

$$\frac{3}{2} V e_d = R_f P + L_f \frac{dP}{dt} - \omega L_f Q + \frac{3}{2} V^2 \quad (30)$$

$$\frac{3}{2} V e_q = R_f Q + L_f \frac{dQ}{dt} + \omega L_f P \quad (31)$$

then, so as to provide decoupled control of reactive power and active power, assuming the output power from the grid side inverter in the synchronous reference frame could be formulated as:

$$\frac{3}{2} V e_d = P_0 - \omega L_f Q + \frac{3}{2} V^2 \quad (32)$$

$$\frac{3}{2} V e_q = Q_0 + \omega L_f P \quad (33)$$

Substitute (30) and (31) into (32) and (33), then:

$$R_f P + L_f \frac{dP}{dt} = P_0 \tag{34}$$

$$R_f Q + L_f \frac{dQ}{dt} = Q_0 \tag{35}$$

P_0 and Q_0 can be completed through defining the power feedback loops as follows:

$$P_0 = K_P\left(P_{ref} - P\right) + K_I \int (P_{ref}\text{-}P)dt \tag{36}$$

$$Q_0 = K_P\left(Q_{ref} - Q\right) + K_I \int (Q_{ref} - Q)dt \tag{37}$$

Where P_{ref} and Q_{ref} are respectively rated active power and rated reactive power. P_{ref} is used in order to maintain a constant output voltage and Q_{ref} is determined by the power factor. We use the voltage regulator with PI control. So, rated active power P_{ref} can be expressed as [12]:

$$P_{ref} = U_{dc}(k_p^{\bullet}(U_{dc-r} - U_{dc}) + k_I^{\bullet}(\int (U_{dc-r} - U_{dc})dt)) \tag{38}$$

Fig.3 shows the control block diagram of grid-side PWM inverter based on the above strategy. There are two closed-loop controls and PWM is used in order to produce the control signal to control the grid-side inverter.

IV. SIMULATION RESULTS

The complete WECS with PMSG was simulated by Matlab/Simulink using the parameters given in Table II. Fig.5 illustrates the waveforms of wind speed and rated wind speed($v_n = 12m/s$). The stator flux reference is 0.192Wb. Fig 6-7-8 and 9 show the waveforms of pitch angle, tip speed ratio, coefficient of power conversion, rotor angular velocity and optimum speed ω_{m-opt}, aerodynamic power. It can be seen that the wind speed increases, rotor angular velocity increases proportionally too, with a limitation due to the pitch angle variation. The power coefficient will drop to maintain the rated output power. Thus, the performance coefficient $C_P$is maintained close their maximum value ($C_{pmax} = 0.41$) until generated power and generator rotor speed exceed rated values. In addition, C_p is decreasing because the operation of the pitch angle control is actuated and the pitch angle β increase if the wind speed is up the rated wind speed ($v_n = 12m/s$). So, rotational speed and power generated are keeping constants. In addition, aerodynamic power is optimized with MPPT strategy and keeps at his nominal value when the wind speed exceeds the nominal value. Fig.8 illustrates the optimum speed and the speed of PMSG. It is seen that the speed follows the optimum quite well. Fig.10 shows the simulation result of DC link voltage that remains a constant value. Therefore, this proves the effectiveness of the established regulators. Fig. 11 shows the simulation results for the stator flux locus. As it's clearly shown, the stator flux follows a predetermined path and as expected, it's trajectory

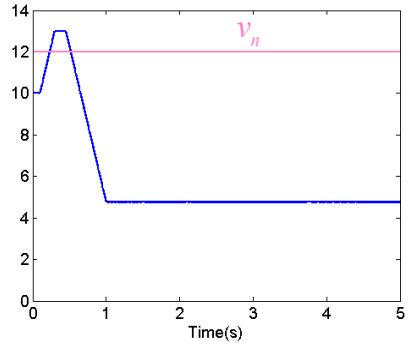

Fig.5. Instantaneous wind speed (m/s)

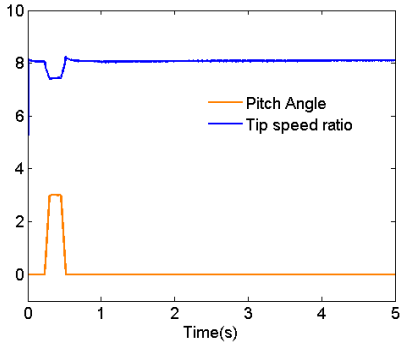

Fig.6. Pitch angle β and λ waveforms.

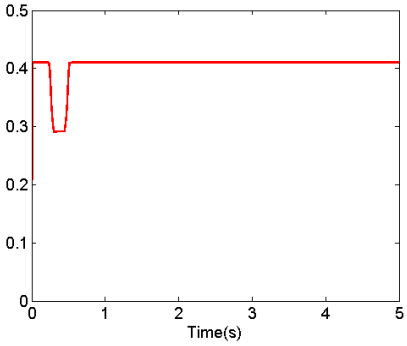

Fig.7. variation of coefficient of power conversion C_p.

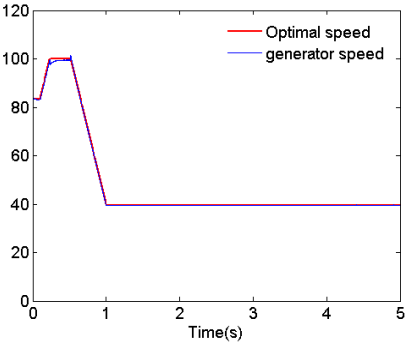

Fig.8. Optimum speed ω_{m-opt} and generator speed ω_m (rd/s).

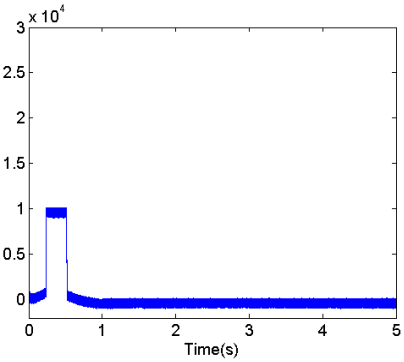

Fig.9. Aerodynamic power (w).

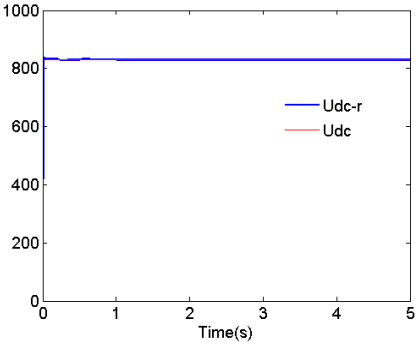

Fig. 10. DC link voltage

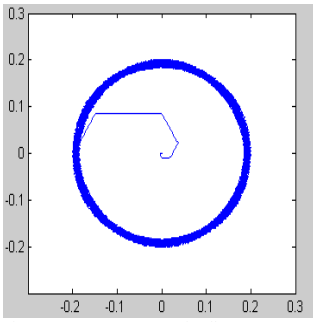

Fig.11. Stator magnetic flux vector trajectory

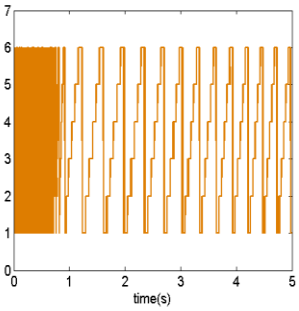

Fig. 12. Sector

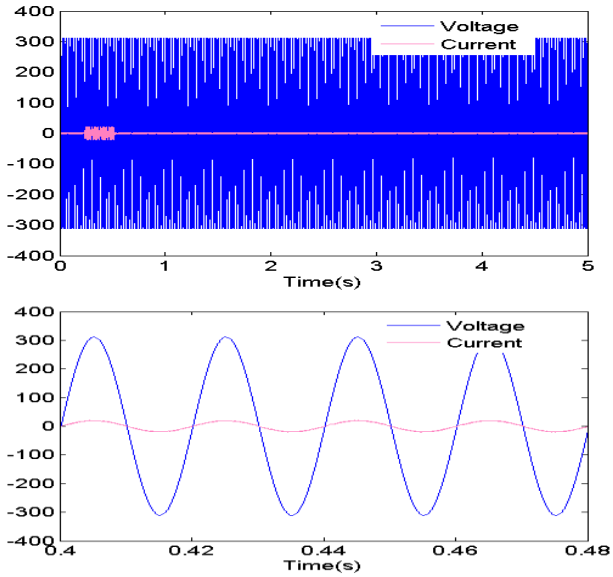

Fig. 13. The waveforms of three phase current and voltage of GRID.

in the stationary reference frame is a circle. Fig. 12 present the sector in which the stator flux is located. Fig.13 shows the variation and a closer observation of three phase current and voltage of GRID. The frequency imposed by the grid is 50 Hz. It's obvious that unity power factor is achieved approximatively. The simulation results demonstrate that the control shows very good dynamic and steady state performance and works very well.

V. CONCLUSIONS

This paper has presented the new control approach of a WECS with variable speed PMSG. The control strategy can implement the concept of MPPT in terms of the adjustment of the PMSG rotor speed according to instantaneous wind speed and can regulate the reactive and active power. So, Control algorithm based on the DTC strategy has been investigated for generator converter but DPC of three phases PWM inverter is adopted and Grid-side reactive and active power decoupling method is applied. As the voltage and frequency of generators outputs vary along the wind speed change, the generator-side converter is used to track the maximum wind power. The employed control strategy can regulate both the reactive and active power independently. The grid side PWM inverter regulates DC-link voltage, injects the generated power into the AC network and it's controlled in order to maintain the frequency and amplitude of the inverter output voltage with unity power factor. The integration of the proposed DTC control of PMSG with the WECS gives satisfying operation characteristics of the wind power generation.

TABLE II
PARAMETERS OF THE POWER SYNCHRONOUS GENERATOR

Parameter	Value
P_r rated power	10 (kW)
$\omega_{...}$ rated mechanical speed	100 (rd/s)
R stator resistance	0.05(Ω)
L_q , L_d stator d-axis and q-axis inductance	0.635 m(H)
$\psi_{.}$ permanent magnet flux	0.192(Wb)
p_n pole pairs	4

REFERENCES

[1] M.A .Abdullah, A.H.M. Yatim, Chee Wei Tan, " A study of maximum power point tracking algorithms for wind energy system", Proceedings of Clean Energy and Technology (CET), IEEE First Conference on, pp. 321 - 326, 2011.

[2] S. M. Muyeen, Rion Takahashi, Toshiaki Murata and Junji Tamura, "A Variable Speed Wind Turbine Control Strategy to Meet Wind Farm Grid Code Requirements", IEEE Transactions on power systems, Vol. 25, No. 1, February 2010, pp. 331 – 340.

[3] Zhe Chen, Josep M. Guerrero and Frede Blaabjerg, "A Review of the State of the Art of Power Electronics for Wind Turbines," IEEE Transactions on power electronics, Vol. 24, No. 8, pp. 1859 - 1875. August 2009.

[4] J.S. Thongam, P. Bouchard, H Ezzaidi, and M Ouhrouche, "Wind speed sensorless maximum power point tracking control of variable speed wind energy conversion systems," Electric Machines and Drives Conference, IEMDC '09. IEEE International, pp. 1832-1837, May 2009.

[5] A. Mesemanolis, C. Mademlis and I. Kioskeridis, "Maximum Efficiency of a Wind Energy Conversion System with a PM Synchronous Generator," IEEE-MedPower 2010, Power Generation, Transmission, Distribution and Energy Conversion, Proceedings of 7th Mediterranean Conference and Exhibition on, pp. 1-9, November 2010.

[6] F. Blaabjerg, F. Iov, Z. Chen, K. Ma, "Power Electronics and Controls for Wind Turbine Systems", Energy Conference and Exhibition (EnergyCon), IEEE Conferences, pp. 333 – 344, December 2010.

[7] S. M. Muyeen, Rion Takahashi and Junji Tamura, "Operation and Control of HVDC-Connected Offshore Wind Farm", IEEE Transactions On Sustainable Energy, Vol. 1, No. 1, pp. 30 – 37, April 2010.

[8] Y. Errami, M. Ouassaid and M. Maaroufi, "Modelling and Control Strategy of PMSG Based Variable Speed Wind Energy Conversion System," Proceedings of IEEE- ICMCS'11, pp. 1-6, 2011.

[9] XiaoHao Zhao, XiaoYun Feng, YongHeng Liao, XinYun Yu and WenSheng Song; "Exploring and modeling on constant speed control strategy of permanent magnet synchronous motor for direct drive system", Electrical Machines and Systems, ICEMS- IEEE International Conference on , pp. 3070 – 3073, 17-20, Oct 2008.

[10] F. Morel, J.-M Retif, Xuefang Lin-Shi, C Valentin, "Permanent Magnet Synchronous Machine Hybrid Torque Control, " IEEE Transactions on Industrial Electronics, Vol. 55 ,No. 2, pp. 501 – 511, February 2008.

[11] B. Singh, B.P Singh and S. Dwivedi, "DSP Based Implementation of Sliding Mode Speed Controller for Direct Torque Controlled PMSM Drive, " Industrial Technology, ICIT-IEEE International Conference on , pp. 1301 - 1308, December 2006.

[12] M.Jasinski,M.P.Kazmierkowski," Sensorless direct power and torque control of PWM back-to-back converter-fed induction motor," Industrial Electronics Society, IECON, 30th Annual Conference of IEEE,Vol.3 ,pp. 2273 – 2278, Nov. 2004 .